Does LoRa Work for Vehicular Networks?

Wenwen Yang and Zijun Gong(✉)

IoT Thrust, HKUST (Guangzhou), Guangzhou, China
wyang018@connect.hkust-gz.edu.cn, gongzijun@hkust-gz.edu.cn

Abstract. The low power wide area network (LPWAN) is the bone of the Internet of Things. As the most successful wireless access technique for LPWAN, LoRa modulation has been widely applied to low mobility or static use cases. But can we use LoRa for high mobility applications, such as outdoor assets or animal tracking? We will answer this question by investigating the possibility of using LoRa in vehicular networks. In LoRa modulation, both propagation delay and Doppler shift can potentially lead to symbol detection errors. Based on our analysis, these two channel parameters are playing very similar roles in deteriorating system performance, and a linear combination of them can be used to quantify how good/bad the channel is. A fundamental tradeoff between signal resilience to delay and Doppler spreads is unveiled, which sheds light on waveform design for LoRa modulation in doubly dispersive channels. This observation is verified through simulations.

Keywords: Chirp signal · LoRa modulation · Delay spread · Doppler spread

1 Introduction

In recent years, the rapid explosion of the Internet of Things (IoT) has revived the research interest in long range communication technologies. Unlike traditional cellular communications that primarily aim to improve spectral efficiency, energy efficiency and communication rate within small cells, IoT requires cost effective and wide area networks. The LoRa (Long Range) is one such technology designed specifically for low power and wide coverage, making it ideal for IoT devices [3].

The application of IoT is wide and diverse, encompassing various scenarios. Some IoT nodes are fixed indoors, and responsible for monitoring, collecting, and transmitting data. Other nodes may be mobile, potentially changing positions as people, vehicles, or other carriers move. The extent to which existing IoT wireless access technologies support node mobility has become a crucial question.

When signals are transmitted through wireless channels with multiple paths, different paths will experience different delays and Doppler shifts, i.e., delay spread and Doppler spread. Larger spreads lead to faster channel variation in time and frequency domains, and add challenges for reliable data detection. There are existing papers talking about the impacts of delay spread [4] and

H.-H. Chen and W. Meng (Eds.): WiSATS 2024, LNICST 605, pp. 338–345, 2025.
https://doi.org/10.1007/978-3-031-86196-3_29

Doppler spread [5] individually. But comprehensive performance evaluation of LoRa modulation in doubly dispersive channels is still missing.

This paper aims to investigate whether LoRa modulation works for vehicular networks, under large delay spread and Doppler spread simultaneously. We will use the symbol error rate (SER) as an evaluation metric [2]. In the following sections, we will first introduce the modulation and demodulation processes in the LoRa protocol. Subsequently, we will analyze the impacts of propagation delay and Doppler shift on the LoRa signals. Finally, we present simulation results to illustrate the system performance of LoRa under various delay and Doppler spread combinations.

2 LoRa Signal Model

2.1 Modulation

The LoRa modulation is a proprietary technique based on the spread spectrum communications technique, for increased communication range with reduced transmit power [1]. The signal spectrum is spread by modulating symbols on chirp signals, and the spreading factor SF is chosen from $\{7, \cdots, 12\}$. For a given spreading factor, there are totally $M = 2^{SF}$ possible symbols. Each symbol is modulated on a waveform of duration T_s, and the maximum instantaneous frequency is given by $B = M/T_s$, with $B \in \{125\,\text{kHz}, 250\,\text{kHz}, 500\,\text{kHz}\}$.

For a symbol $a \in \{0, 1, \cdots, M-1\}$, the instantaneous frequency starts at f_a and increases linearly at a rate of B/T_s until it reaches B. The instantaneous frequency will then be wrapped to 0 and continue to increase linearly at a rate of B/T_s. The instantaneous frequency of symbol a in a symbol duration can be written as

$$f_a(t) = \text{mod}\left(a\frac{B}{M} + \frac{B}{T_s}t, B\right). \tag{1}$$

Figure 1 illustrates the instantaneous frequency of the waveform corresponding to symbol a in the LoRa modulation. The instantaneous frequency reaches the maximum B at $t_a = T_s\left(1 - \frac{a}{M}\right)$. The instantaneous phase can be calculated by integrating the instantaneous frequency, given by

$$\phi_a(t) = 2\pi \int_0^{T_s} f_a(\tau)d\tau = \begin{cases} 2\pi\left(a\frac{B}{M}t + \frac{1}{2}\frac{B}{T_s}t^2\right), & 0 \le t \le t_a \\ 2\pi\left(a\frac{B}{M}t + \frac{1}{2}\frac{B}{T_s}t^2 - Bt\right), & t_a < t \le T_s \end{cases}. \tag{2}$$

The waveform of the modulated signal can be expressed as

$$s_a(t) = e^{j2\pi\phi_a(t)} = \begin{cases} e^{j2\pi Bt\left(\frac{a}{M} + \frac{1}{2}\frac{t}{T_s}\right)}, & 0 \le t \le t_a \\ e^{j2\pi Bt\left(\frac{a}{M} + \frac{1}{2}\frac{t}{T_s} - 1\right)}, & t_a < t \le T_s \end{cases}. \tag{3}$$

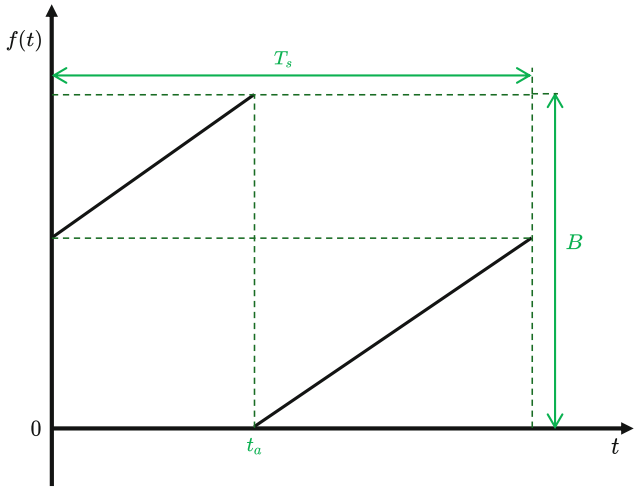

Fig. 1. LoRa signal representation.

2.2 Demodulation

As LoRa is a proprietary technology, its technical details have not been fully disclosed [6], and we don't know exactly how LoRa signals are demodulated in commercial LoRa chips. Nonetheless, many possible ways for demodulation can be found in the literature [7]. In this paper, we will focus on the maximum likelihood (MLE) detector.

For the additive white Gaussian noise channel, the received signal is

$$r(t) = s_a(t) + w(t), \tag{4}$$

where $w(t) \sim \mathcal{CN}(0, \sigma^2)$ is a zero mean complex white Gaussian noise. Then the received signal is correlated with the reference signal $s_0^*(t) = e^{-j2\pi\frac{1}{2}\frac{B}{T_s}t^2}$ to get the detection signal $d(t)$

$$d(t) = r(t)s_0^*(t) = \begin{cases} e^{j2\pi Bt\frac{a}{M}} + \tilde{w}(t), & 0 \le t \le t_a \\ e^{j2\pi Bt\left(\frac{a}{M}-1\right)} + \tilde{w}(t), & t_a < t \le T_s \end{cases}, \tag{5}$$

where $\tilde{w}(t) = w(t)s_0^*(t)$.

Then we can discretize the signal $d(t)$ with a sampling interval of $T = 1/B$, and the sampled sequence is

$$d[n] = d(nT) = e^{j2\pi a\frac{n}{M}} + \tilde{w}[n], \tag{6}$$

where $\tilde{w}[n] = \tilde{w}(nT)$. This is a discrete complex sinusoid contaminated by white noise, and our goal is to estimate a. This can be done by computing the discrete

Fourier transform (DFT) of $d[n]$ as

$$\begin{aligned} D[k] &= \sum_{n=0}^{M-1} d[n] e^{-j2\pi k \frac{n}{M}} \\ &= \frac{1 - e^{j2\pi(a-k)}}{1 - e^{j2\pi\left(\frac{a}{M} - \frac{k}{M}\right)}} + \tilde{W}[k] \\ &= M\delta(k-a) + \tilde{W}[k], \end{aligned} \tag{7}$$

where $\tilde{W}[k] = \sum_{n=0}^{M-1} \tilde{w}[n] e^{-j2\pi k \frac{n}{M}}$ is the DFT of the noise and $\delta(\cdot)$ is a Dirac delta function, defined as

$$\delta(t) = \begin{cases} 1, t = 0 \\ 0, t \neq 0 \end{cases}. \tag{8}$$

The symbol detection is then conducted by $\hat{a} = \arg\max_k |D[k]|$. The magnitude $|D[k]|$ is thus given by

$$|D[k]| = \begin{cases} M + \tilde{W}[a], k = a \\ \tilde{W}[k], \quad\quad k \neq a \end{cases}. \tag{9}$$

As we can see, the LoRa modulation is reliable in ideal wireless channels, with no delay or Doppler spread. In the following section, we will investigate the impact of doubly dispersive channels on LoRa signals.

3 LoRa Signal in Doubly Dispersive Channels

In general, the delay and Doppler spread deform communication signals in very different ways. However, they will manifest themselves on LoRa signals with similar consequences. It turns out that the LoRa signals have limited capacities for distortion resilience, shared by both delay and Doppler spreads. We will first investigate the impacts of delay and Doppler shift on LoRa signals, and then consider them jointly.

3.1 Impact of Doppler Shift

When there is a relative velocity between the transmitter and the receiver, the received signal frequency will change, resulting in a Doppler shift. The received signal with Doppler shift ν is

$$r_d(t) = e^{j2\pi\nu t} s_a(t) + w(t). \tag{10}$$

The instantaneous frequency of the signal will thus be changed by ν Hz, resulting in a vertical shift demonstrated in Fig. 2. A positive Doppler shift causes the signal to move upward, while a negative one leads to a downward shift. This shift will boost the possibility of incorrect decisions in symbol detection.

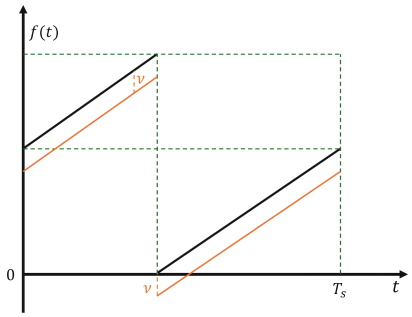

Fig. 2. Impact of Doppler shift.

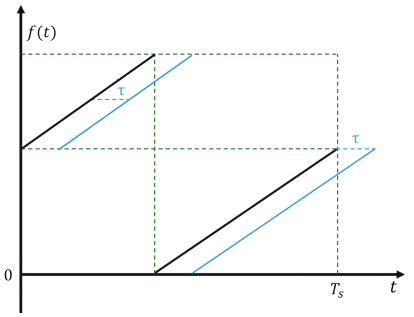

Fig. 3. Impact of propagation delay.

The detection signal will also be shifted by ν Hz in this case, and the DFT of the sampled detection signal is given by

$$D_d[k] = e^{-j2\pi B\tau} \sum_{n=0}^{M-1} e^{-j2\pi \frac{n}{M}(k-(a+\nu T_s))} + \tilde{W}[k]. \tag{11}$$

When νT_s is exactly an integer, the peak of the spectrum will be identified as $k = a + \nu T_s$, leading to a symbol detection error. The distance between two symbols in the frequency domain is B/M, and a Doppler shift of $B/M/2$ will significantly deteriorate the system performance.

3.2 Impact of Propagation Delay

The received signal with a propagation delay τ is given as

$$r_p(t) = s_a(t-\tau) + w(t). \tag{12}$$

A propagation delay leads to a horizontal shift of the instantaneous frequency, depicted in Fig. 3, leading to an increased detection error rate.

The detection signal will also experience a delay of τ. We can then get the DFT of the sampled detection signal as

$$\begin{aligned} D_p[k] = e^{-j\theta_1} &\sum_{n=0}^{M-a+\lfloor B\tau \rfloor} e^{j2\pi \frac{n}{M}(a-B\tau-k)} \\ &+ e^{-j\theta_2} \sum_{M-a+\lfloor B\tau \rfloor+1}^{M-1} e^{j2\pi \frac{n}{M}(a-B\tau-k)} + \tilde{W}[k], \end{aligned} \tag{13}$$

where $\theta_1 = 2\pi B\tau \left(\frac{a}{M} - \frac{\tau}{2T_s}\right)$ and $\theta_2 = 2\pi B\tau \left(\frac{a}{M} - \frac{\tau}{2T_s} - 1\right)$. Both θ_1 and θ_2 are the phase factors independent of n and we are only concerned with the magnitude of $|D_p[k]|$. So we can simplify the expression

$$|D_p[k]| = \left| \sum_{n=0}^{M-1} e^{-j2\pi \frac{n}{M}(k-(a-B\tau))} + \tilde{W}[k] \right|. \tag{14}$$

The propagation delay will cause a shift of the spectrum of the detection signal, leading to increased symbol detection error rate. Similar to the case of the Doppler shift, when $a - B\tau$ is an integer, the peak value is obtained at $k = a - B\tau$.

Interestingly, a propagation of τ will approximately lead to a peak shift of τB in the spectrum of detection signal. Recall that a Doppler shift of ν means a peak shift of νT_s in the spectrum shift. The delay and Doppler shift are actually playing very similar roles in deteriorating system performance.

3.3 Joint Impact of Delay and Doppler

Consider a doubly dispersive channel with L propagation paths, and the received signal will be

$$r(t) = A_0 s_a(t) + \sum_{l=1}^{L-1} A_l e^{-j2\pi\nu_l(t-\tau_l)} s_a(t-\tau_l) + w(t). \tag{15}$$

where A_l, ν_l and τ_l are the overall attenuation, propagation delay and Doppler shift in the l-th path.

After the correlation and sampling, we can get the DFT of the detection signal as

$$D[k] = MA_0\delta(k-a) + \sum_{l=1}^{L-1} \tilde{A}_l \sum_{n=0}^{M-1} e^{j2\pi\frac{n}{M}(a-B\tau_l-T_s\nu_l-k)} + \tilde{W}[k], \tag{16}$$

where $\tilde{A}_l = A_l e^{2\pi B\frac{\tau_l}{M}(a-B\tau_l/2-\nu_l T_s)}$. Clearly, Doppler shift and propagation delay lead to a peak shift of $\tau_l B + \nu_l T_s$. A larger shift means an increased possibility of symbol detection error rate. For two different combinations of delay and Doppler shift, i.e., (τ_1, ν_1) and (τ_2, ν_2), as long as $\tau_1 B + \nu_1 T_s = \tau_2 B + \nu_2 T_s$, the overall impact on system performance will be approximately the same. This is visually demonstrated in Fig. 4.

4 Simulation Results

In this section, we present the simulation results obtained using MATLAB to evaluate the performance of LoRa modulation under various conditions. Figure 5 illustrates the performance of different spreading factors under an AWGN channel. Figure 6 demonstrates the performance characteristics for a bandwidth of 125 kHz and a spreading factor of 8, where the combination of delay and Doppler shifts maintains a constant value of 0.35. It can be observed that the performance of the signal remains the same for different combinations of delay and Doppler, validating our previous assertion.

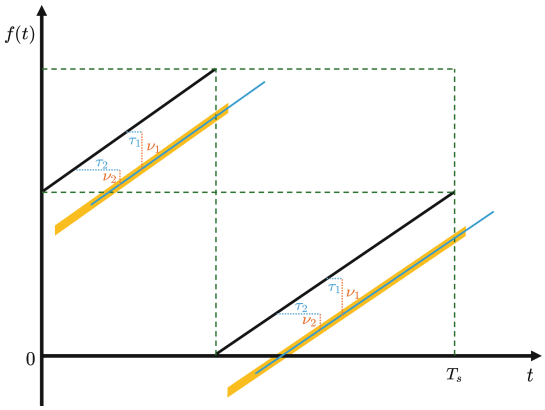

Fig. 4. Different groups of delay and Doppler.

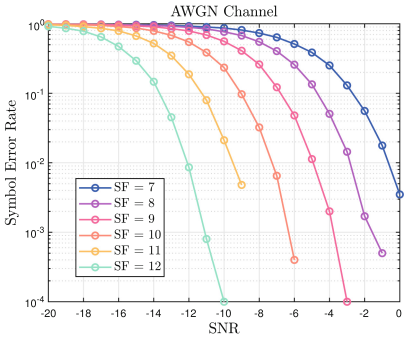

Fig. 5. Performance of different spreading factors under AWGN channel.

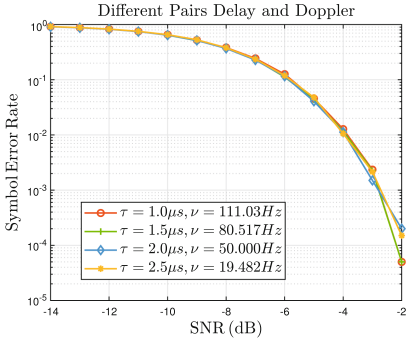

Fig. 6. Constant impact of different delay and Doppler.

5 Conclusion and Future Work

In this paper, we investigated the feasibility of LoRa modulation in vehicular networks, focusing on the impacts of propagation delay and Doppler shift. The primary goal was to assess whether LoRa could maintain reliable communication performance under typical vehicular conditions. We analyzed the effects of delay and Doppler separately. Our analysis shows that the impact of delay and Doppler on signal demodulation is similar. A metric is identified to quantify the overall impact of delay spread and Doppler spread, which is confirmed by our simulation results. In future work, we will consider adjust the modulation parameter like spreading factor and bandwidth in order to enhance the robustness and reliability of LoRa modulation in vehicular networks.

Acknowledgement. Z. Gong is the corresponding author. This work was supported in part by the National Natural Science Foundation of China (62201162); in part by

the Guangzhou-HKUST(GZ) Joint Funding Scheme (2023A03J0132); in part by the Guangzhou Basic and Applied Basic Research Scheme (2024A04J4303); in part by the Guangdong Provincial Key Lab of Integrated Communication, Sensing and Computation for Ubiquitous Internet of Things (2023B1212010007); in part by Guangzhou Municipal Science and Technology Project (2023A03J0011).

References

1. Adelantado, F., Vilajosana, X., Tuset-Peiro, P., Martinez, B., Melia-Segui, J., Watteyne, T.: Understanding the limits of LoRaWAN. IEEE Commun. Mag. **55**(9), 34–40 (2017). https://doi.org/10.1109/MCOM.2017.1600613
2. Afisiadis, O., Cotting, M., Burg, A., Balatsoukas-Stimming, A.: On the error rate of the LoRa modulation with interference. IEEE Trans. Wireless Commun. **19**(2), 1292–1304 (2019)
3. Centenaro, M., Vangelista, L., Zanella, A., Zorzi, M.: Long-range communications in unlicensed bands: the rising stars in the IoT and smart city scenarios. IEEE Wirel. Commun. **23**(5), 60–67 (2016). https://doi.org/10.1109/MWC.2016.7721743
4. Demeslay, C., Rostaing, P., Gautier, R.: Theoretical performance of LoRa system in multipath and interference channels. IEEE Internet Things J. **9**(9), 6830–6843 (2021)
5. Petäjäjärvi, J., Mikhaylov, K., Pettissalo, M., Janhunen, J., Iinatti, J.: Performance of a low-power wide-area network based on LoRa technology: doppler robustness, scalability, and coverage. Int. J. Distrib. Sens. Netw. **13**(3), 1550147717699412 (2017)
6. Seller, O.B.A., Sornin, N.: Low power long range transmitter. U.S. Patent US9252834B2 (2016). assigned to Semtech Corporation. https://patents.google.com/patent/US20140219329A1/en
7. Vangelista, L.: Frequency shift chirp modulation: the LoRa modulation. IEEE Signal Process. Lett. **24**(12), 1818–1821 (2017)